

Passive Sensors for Infrastructure Monitoring

Sharon L. Wood^{*a} and Dean P. Neikirk^b

^a Department of Civil, Architectural & Environmental Engineering, Univ. of Texas,
Austin, TX, USA 78712

^b Department of Electrical and Computer Engineering, Univ. of Texas, Austin, TX, USA 78712

ABSTRACT

A class of low-cost, wireless sensor has been developed at the University of Texas at Austin to monitor the performance of reinforced and prestressed concrete members in civil infrastructure systems. The sensors are designed to be interrogated in a wireless manner as part of a routine inspection. The sensors do not require batteries or connections to external power supplies. As such, the sensors are intended to be maintenance free over the service life of the infrastructure system.

Research efforts to date have focused on detecting the onset of corrosion. It is envisioned that the sensors would be attached to the reinforcement cages before placement of the concrete. The results of long-term exposure tests will be used in this presentation to demonstrate the potential and reliability of the resonant sensors.

Keywords: corrosion detection, reinforced concrete structures, embedded sensors, passive sensors, threshold sensors, exposure tests

1. INTRODUCTION

The development of comprehensive, health monitoring systems for civil infrastructure is an extremely challenging problem. Each civil infrastructure system is unique, exposed continuously to the environment, designed for a service life of many decades, very large in scale, and susceptible to damage from many sources. While health monitoring systems have been installed on several signature bridges in the US^{1,2}, the costs associated installing, maintaining, and interpreting the data are prohibitively expensive for the overwhelming majority of civil infrastructure systems. In stark contrast to comprehensive, real-time sensor networks, the passive sensors discussed in this paper provide a cost-effective option for enhancing the type and quality of information that can be obtained about the condition of an infrastructure system. The sensors were designed to satisfy the following three objectives: low cost, long life, and reliable output. It is envisioned that the sensors will be embedded in a structure during construction and interrogated sporadically over the service life as part of routine inspections. The sensors are powered and interrogated wirelessly using inductively coupled magnetic fields. Without the need for batteries, the expected life of the sensors is the same as the design life of the bridge.

The sensors discussed in this paper provide an economic, nondestructive means of evaluating the environmental conditions within a reinforced concrete structure. To date, the research team has focused on detecting the initiation of corrosion³⁻⁶. A prototype resonant corrosion sensor has been developed to detect a threshold level of corrosion, which occurs well before the onset of structural damage. The results of long-term exposure tests are used in this paper to evaluate the sensitivity of the sensor reading to variations in the environmental conditions within the concrete (temperature, humidity, and moisture levels).

* swood@mail.utexas.edu; phone 1 512 471-7298; fax 1 512 471-1944

2. THRESHOLD CORROSION SENSOR

The wireless sensor platform developed at the University of Texas comprises two basic parts: a passive, resonant sensor that is embedded in the concrete and an external reader coil (Fig. 1a). The external reader coil is magnetically coupled to an inductive coil in the sensor. This reader coil is used to both power and interrogate the sensor.

The passive sensors rely on the resonant characteristics of RLC circuits to transmit information about the conditions within the concrete structure. The frequency response of an RLC circuit can be determined by measuring the vector impedance across the terminals of the external reader coil (Fig. 1b). The resonant frequency of the RLC circuit corresponds to a minimum in the phase of the impedance (Fig. 1c) and the value of the resonant frequency depends on the values of the inductance, L_2 , and capacitance, C_2 , of the resonant circuit:

$$f = \frac{1}{2\pi} \sqrt{\frac{1}{L_2 \cdot C_2}} \quad (1)$$

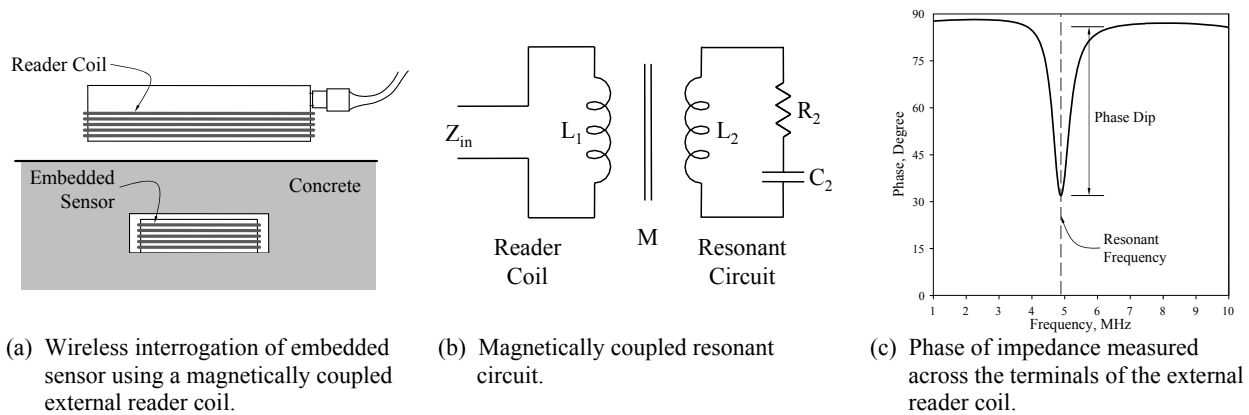


Figure 1: Wireless interrogation of resonant sensors.

The difference between the amplitude of the phase response away from the resonant frequency and the amplitude at the resonant frequency is called the phase dip, and depends on the coupling efficiency between the reader coil and the coil in the resonant circuit and resistance of the RLC circuit. As the resistance, R_2 , increases, the amplitude of the phase dip decreases. The prototype, threshold corrosion sensor includes two resonant circuits. The sensing circuit includes a transducer mechanism – a steel sensing wire that extends into the concrete and is exposed to the same levels of oxygen, moisture, and chlorides as the adjacent reinforcement. The second circuit serves only as a reference.

The circuit diagram for the prototype corrosion sensor is shown in Fig. 2a. The steel sensing wire was placed in series with the inductor and capacitor in the sensing circuit and has been idealized as a switch. A photograph of the prototype corrosion sensor is shown in Fig. 2b. The circuit components were embedded in marine epoxy to protect the sensor from damage during placement of the concrete and to minimize exposure to the high pH environment within the concrete. If the steel sensing wire is exposed to chlorides within the concrete, corrosion will cause the sensing wire to fracture (Fig. 2c). In the absence of chlorides, the passive layer that forms on the surface of steel embedded in concrete protects the reinforcement from corrosion.

As shown in Fig. 2b, the two inductive coils are positioned concentrically in the prototype corrosion sensor. The larger diameter coil is part of the sensing circuit, and the smaller coil is part of the reference circuit. Before the onset of corrosion, the resonant frequencies of both the sensing and reference circuits are clearly visible when the sensor is interrogated (Fig. 3a). The capacitance of each circuit was selected such that the two resonant frequencies were well separated. When the steel wire fractures due to corrosion, the switch in the sensing circuit opens and the resonant frequency of the sensing circuit can no longer be detected (Fig. 3b). In addition, the resonant frequency of the reference circuit shifts slightly lower and the phase dip increases.

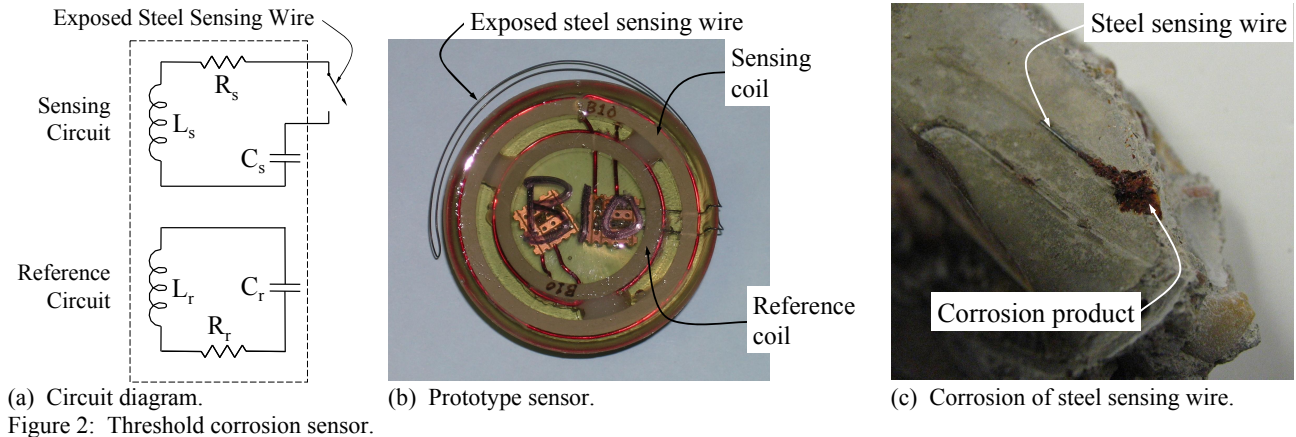
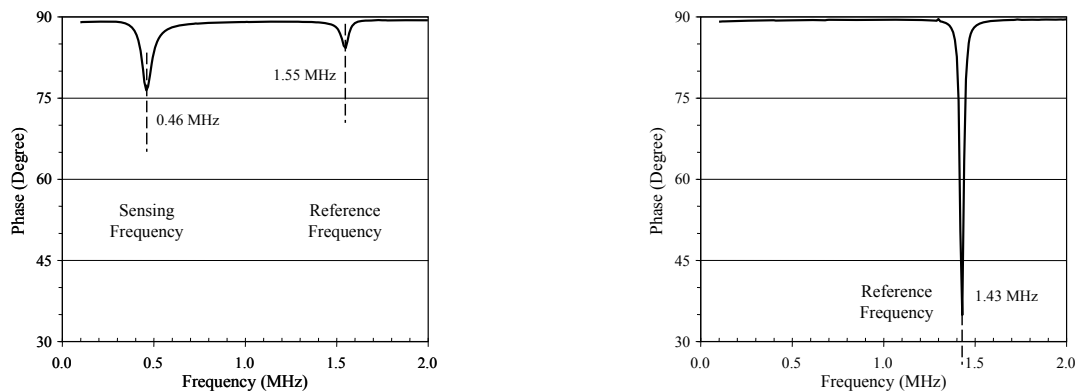


Figure 2: Threshold corrosion sensor.

In reality, the resistance of the wire increases – and the amplitude of the phase dips decreases – as the steel sensing wire corrodes. However, the diameter of the sensing wire is so much smaller than the deformed reinforcement that corrosion will cause the sensing wire to fracture before appreciable structural damage has occurred in the reinforcement. Therefore, the sensing wire can be idealized as a switch and the sensor can be idealized as a threshold sensor. If two resonant frequencies are present when a sensor is interrogated, the likelihood of corrosion at the location of the sensor is low. In contrast, if only one resonant frequency is present, the likelihood of corrosion is high.



(a) Before corrosion of sensing wire – both sensing and reference circuits are detected.

(b) After corrosion of sensing wire – only reference circuit is detected.

Figure 3: Phase response of prototype corrosion sensor.

3. LONG-TERM EXPOSURE TESTS

The long-term performance of the prototype sensors was monitored during environmental exposure tests. Sensors were embedded in four, reinforced concrete test specimens and interrogated periodically during the tests. The primary objective was to determine if the threshold corrosion sensors provided reliable information about the onset of corrosion within reinforced concrete members. Data from the tests were also used to evaluate the sensitivity of the sensor readings to changes in environmental conditions, such as temperature and moisture content of the concrete, and to determine if the switch in the threshold corrosion sensor would remain open after corrosion occurs. It is essential that the sensor readings not alternate between the open and closed states once the onset of corrosion is detected.

The test specimens (Fig. 4 and 5) were selected to represent portions of a bridge deck. The specimens were 8 in. deep, 18 in. wide, and 10 ft long. Two, #5 bars were used as the top layer of reinforcement and six, #3 bars were used as the bottom layer (Fig. 5). Clear cover to the top reinforcement was approximately 1 in. in all specimens. The slabs were subjected to sustained, concentrated loads near the ends, creating a 3-ft region of constant negative moment between the supports (Fig. 4).

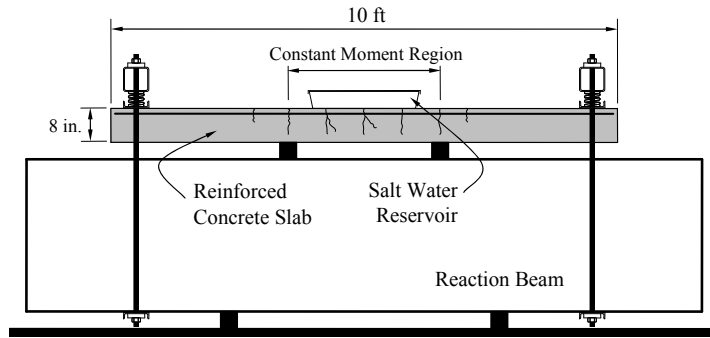


Figure 4: Elevation of test specimens used for long-term exposure test.

The nominal dimensions and longitudinal reinforcement in all four specimens were the same, but there were several important differences between Slabs 1 and 2 and Slabs 3 and 4:

- Deformed #3 bars were used as the transverse reinforcement in Slabs 1 and 2.
- Pairs of plain W5 wire were used as the transverse reinforcement in Slabs 3 and 4.
- The top and bottom layers of reinforcement were electrically isolated in Slabs 1 and 2 to minimize the likelihood of macrocell corrosion. The two layers of reinforcement were supported independently on plastic chairs (Fig. 6).
- The top and bottom layers of reinforcement were supported independently on the transverse reinforcement in Slabs 3 and 4 (Fig. 7). One top bar and both bottom bars extended beyond the formwork (Fig. 8). The ends of the transverse bars were covered to prevent corrosion from the atmosphere⁷. The layers of transverse reinforcement were connected using five, 100-Ω resistors along the length of the specimen to facilitate the development of macrocell corrosion.

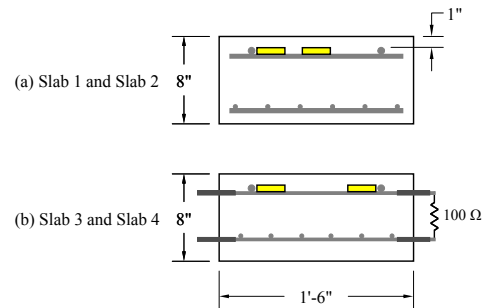


Figure 5: Cross section of test specimens used for long-term exposure test.

The chemical and physical properties of the steel reinforcement and steel sensing wires used in all four specimens are summarized in Table 1.



Figure 6: Plastic chairs were used to support the layers of reinforcement independently in Slabs 1 and 2.



Figure 7: Top and bottom layers of reinforcement were supported independently on the transverse reinforcement in Slabs 3 and 4.



Figure 8: Layers of transverse reinforcement extended beyond the concrete in Slabs 3 and 4.

The specimens were cracked in flexure at the start of the exposure tests. The average crack widths within the constant moment regions for Slabs 1 and 2 were 0.02 in. Average crack widths within the constant moment regions for Slabs 3 and 4 were 0.01 in. Cracks extended across the entire width of the top surface of the slab in all specimens.

A 24-in. by 14-in. plastic reservoir was positioned at midspan of each slab, which was periodically filled with salt water. A four-week moisture cycle was selected: the reservoir was filled with salt water two weeks and the concrete was allowed to dry for the next two weeks. The sensors were interrogated at the end of each two-week period. The salt water contained 3.5% NaCl by weight. The slabs were stored in an unheated building and experienced temperature fluctuations of more than 70 °F during the tests. The salt water reservoirs provided the only source of moisture for the slabs, other than humidity in the atmosphere.

Table 1: Chemical and physical properties of reinforcement and steel sensing wire

Property	Deformed Reinforcement	W5 Wire	Steel Sensing Wire		
			Slab 1	Slab 2	Slabs 3 and 4
Diameter, in.	—	—	0.0159	0.0285	0.0285
Gage	—	—	26	21	21
AISI-ASE Designation	—	—	1005	1006	1060
Carbon, %	0.38	0.11	0.04	0.05	0.60
Manganese, %	0.89	0.60	0.22	0.38	0.78
Phosphorus, %	0.021	0.015	0.005	0.015	0.018
Sulfur, %	0.036	0.040	0.019	0.024	<0.005
Silicon, %	0.26	0.15	<0.01	0.04	0.23
Nickel, %	0.13	0.05	0.04	0.04	0.06
Chromium, %	0.16	0.01	<0.01	0.01	0.06
Molybdenum, %	0.04	0.01	<0.01	<0.01	<0.01
Copper, %	0.33	0.03	0.02	0.01	0.09
Aluminum, %	—	—	—	—	0.009

Within each test specimen, sensors were positioned in three regions: beneath the salt water reservoir, near the ends of the slab, and in the transition region adjacent to the salt water reservoir (Fig. 9). The risk of corrosion was considered to be highest directly below the salt water reservoir due to the presence of chloride ions. During the tests, moisture from the reservoir spread approximately 20 in. on either side of midspan due to the permeability of the concrete. Therefore, the risk of corrosion was considered to be lowest near the ends of the slab (45 in. from midspan). In Slabs 1 and 2, the sensors in the transition region (18 in. from midspan) experienced moisture fluctuations. However, the sensors in the transition region (22.5 in. from midspan) in Slabs 3 and 4 remained dry throughout the exposure tests.

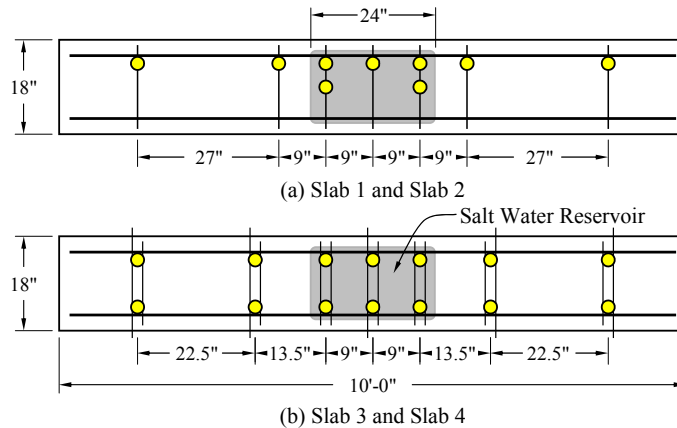


Figure 9: Layout of threshold corrosion sensors in test specimens.

Detailed information about the sensors in each test specimen is summarized below:

- Nine threshold corrosion sensors (Fig. 9a) were supported on the top layer of reinforcement in Slabs 1 and 2. The sensors in Slab 1 were fabricated using 26-gage steel wire and the sensors in Slab 2 were fabricated using 21-gage steel wire. Sensing wires were not attached to the top layer of reinforcement (Fig. 10).

- Eight corrosion sensors of an alternate design were also embedded in Slabs 1 and 2 (shown on the right side of Fig. 6). The sensing and reference coils were adjacent in this design, but the amplitude of the measured response was considerably lower for this configuration. This arrangement of coils was subsequently rejected⁸; therefore, the response of the sensors with adjacent coils is not addressed in this paper.
- Fourteen threshold corrosion sensors (Fig. 9b) were attached to the top layer of reinforcement in Slabs 3 and 4. All sensors were fabricated using 21-gage steel wire. Sensing wires were attached to the top layer of reinforcement (Fig. 11).
- Four analog conductivity sensors and five thermocouples were also embedded in Slabs 3 and 4 (shown in the center of Fig. 7). The response of these sensors is discussed elsewhere^{9,10} and is beyond the scope of in this paper.

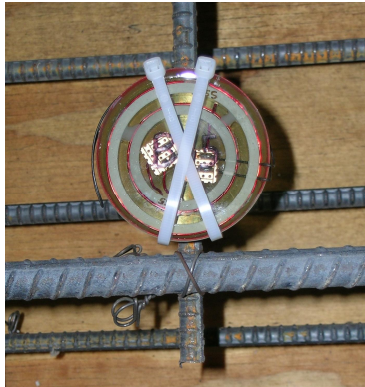


Figure 10: Steel sensing wires were not connected to the top layer of reinforcement in Slabs 1 and 2.

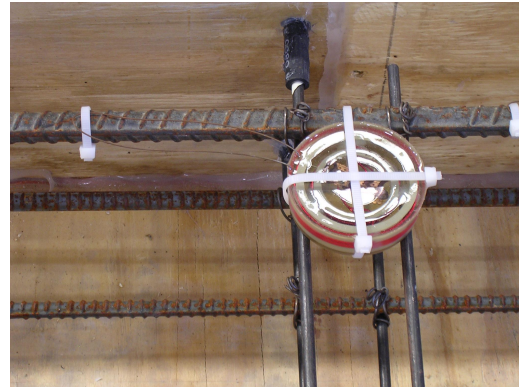


Figure 11: Steel sensing wires were connected to the top layer of reinforcement in Slabs 3 and 4.

The response of the threshold corrosion sensors from the four slabs are summarized in this paper. Slabs 1 and 2 were constructed in December 2004 and exposed to periodic moisture cycles between January 2005 and June 2006. Slabs 3 and 4 were cast in March 2006. Slab 4 was subjected to periodic moisture cycles between April 2006 and April 2007. The duration of the exposure test was longer for Slab 3, which was subjected to periodic moisture cycles between April 2006 and November 2007 and intermittent moisture cycles between November 2007 and September 2008.

Slabs 1, 2, and 4 were demolished at the conclusion of the exposure tests to determine the extent of corrosion within the specimens. Corrosion was observed on the surface of the longitudinal reinforcement in the regions of the specimens that experienced moisture fluctuations. Corrosion levels were highest in the immediate vicinity of the flexural cracks (Fig. 12). Slab 3 is scheduled to be demolished in the next few months.



(a) Slab 1



(b) Slab 2

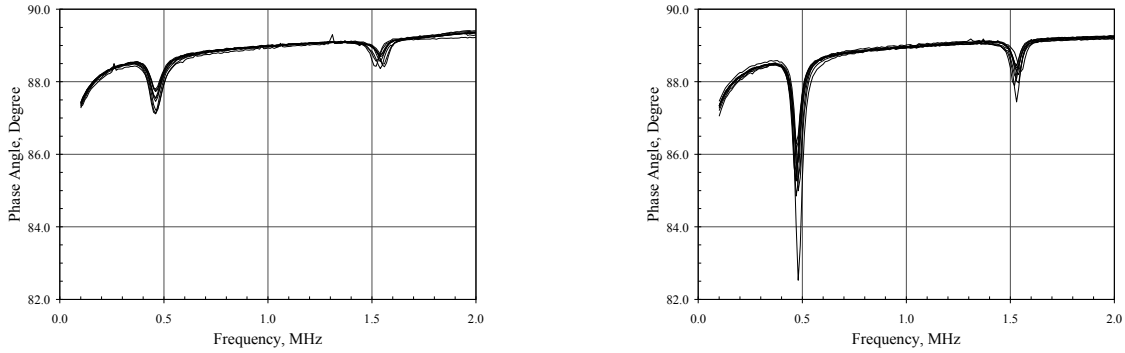


(c) Slab 4

Figure 12: Condition of longitudinal reinforcement at conclusion of long-term exposure test.

4. MEASURED RESPONSE OF THRESHOLD SENSORS

The measured frequency response of the sensors embedded in Slabs 1 and 2 are plotted in Fig. 13. Measurements were taken immediately before the specimens were exposed to salt water in the first wet/dry cycle. Two resonant frequencies are clearly visible in all curves, indicating that the steel sensing wires were sufficiently robust to survive the construction process. The amplitudes of the phase dips for the sensors in Slab 1 were less than those for the sensors in Slab 2 due to the higher resistance of the smaller diameter steel sensing wire.



(a) Slab 1 (b) Slab 2
 Figure 13: Response of sensors embedded in Slabs 1 and 2 at beginning of long-term exposure test.

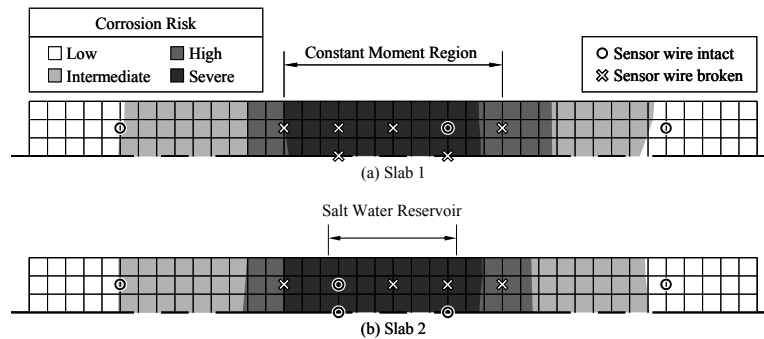


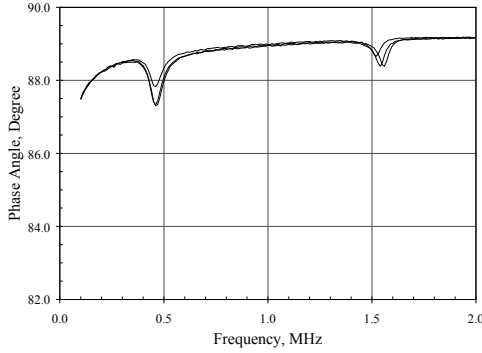
Figure 14: Contour plots of corrosion risk based on half-cell potentials and condition of sensors embedded in Slabs 1 and 2 at conclusion of long-term exposure test.

During the exposure test, half-cell potentials were used to identify the regions of the test specimens where corrosion was most likely to occur. The contour plots of corrosion risk, based on the half-cell readings at the conclusion of the exposure test, are plotted in Fig. 14 for Slabs 1 and 2. As expected, the half-cell potentials were highest directly below the salt water reservoir and were lowest at the ends of the slabs. The condition of the sensors at the conclusion of the exposure tests is also indicated in Fig. 14. In Slab 1, the steel sensing wires corroded in six of the seven sensors located in regions of high and severe corrosion risk and the steel sensing wires were intact in both sensors located in regions of low corrosion risk (Fig. 15). The results were similar in Slab 2, where four of seven sensors located in regions of high and severe corrosion risk indicated the likelihood of corrosion (Fig. 16).

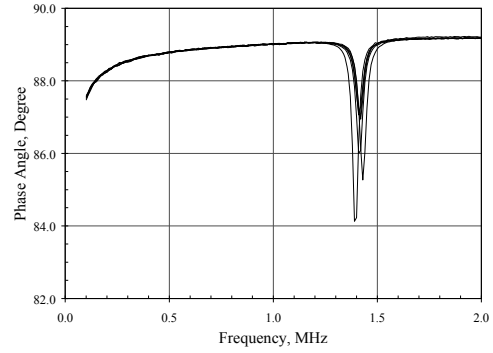
It is important to note that the half-cell potential readings were sensitive to the moisture content of the concrete. Fluctuations of more than 150 mV were observed in consecutive readings at the same location between the wet and dry cycles. In contrast, once a threshold sensor detected the onset of corrosion, that sensor displayed a single resonant frequency in all subsequent interrogations. Therefore, the response of the sensors was not sensitive to the moisture content or the temperature of the concrete.

As shown in Fig. 12, corrosion was observed on the surface of the longitudinal and transverse reinforcement when the concrete cover was removed after the conclusion of the exposure test. However, the surface of the reinforcement was not uniformly corroded; the corrosion was concentrated in the immediate vicinity of the flexural cracks indicating that local anodes and cathodes had formed along the reinforcement. This indicates that the initiation of corrosion was a local phenomenon in Slabs 1 and 2, where the two layers of reinforcement were electrically isolated.

The observation that initiation of corrosion is not uniform represents a challenge for the threshold sensors. Even in regions of nominally identical corrosion risk, the sensing wires did not always cross the path of the flexural crack. Therefore, the time needed for the chlorides to reach the sensing wire and cause corrosion varied significantly within the same test specimen, and several sensors that were located in the region of highest corrosion risk (Fig. 14) did not indicate the likelihood of corrosion.

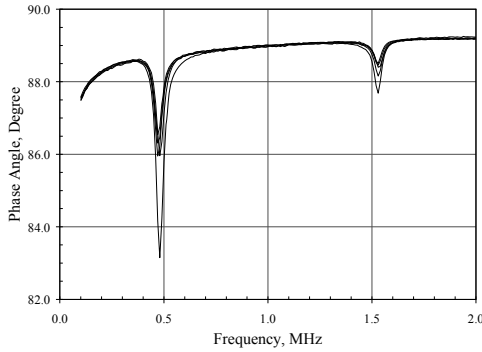


(a) Three sensors with intact sensing wires

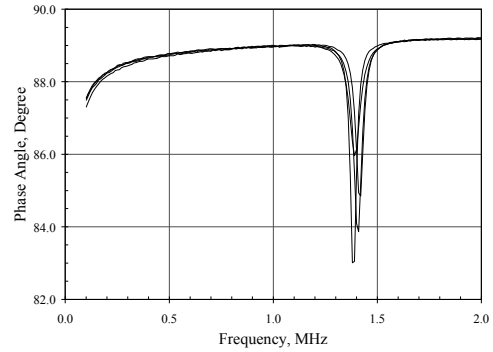


(b) Six sensors with corroded sensing wires

Figure 15: Response of sensors embedded in Slab 1 at conclusion of long-term exposure test.



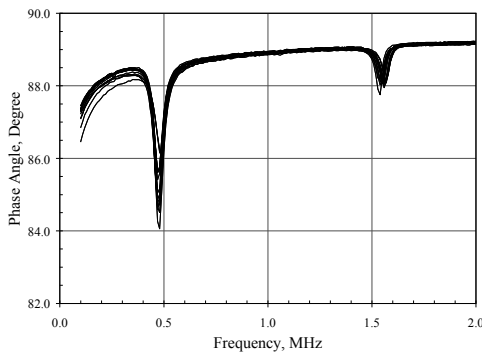
(a) Five sensors with intact sensing wires



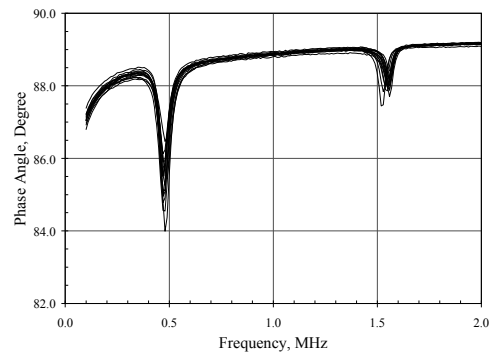
(b) Four sensors with corroded sensing wires.

Figure 16: Response of sensors embedded in Slab 2 at conclusion of long-term exposure test.

Slabs 3 and 4 differed from Slabs 1 and 2 in two ways: (1) the top and bottom layers of reinforcement were connected in Slabs 3 and 4 to induce macrocell corrosion and (2) the steel sensing wires were attached to the top layer of reinforcement in Slabs 3 and 4 in an attempt to increase the tributary area of the sensors. As shown in Fig. 17, the electrical connection between the steel sensing wires and the top layer of reinforcement did not influence the initial frequency response of the sensors.



(a) Slab 3



(b) Slab 4

Figure 17: Response of sensors embedded in Slabs 3 and 4 at beginning of long-term exposure test.

However, the electrical connection between the top and bottom layers of reinforcement did accelerate the formation of corrosion within the test specimens. As shown in Figure 18, corrosion stains were observed on the top surface of Slabs 3 and 4 within the first several months of the exposure tests. As a result, the exposure test for Slab 4 was concluded after one year.

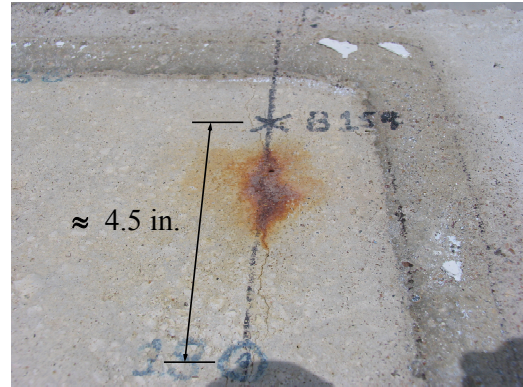


Figure 18: Evidence of corrosion on top surface of Slab 4 after one year.

In April 2007 only two of the threshold sensors had detected the onset of corrosion in each of the slabs (Fig. 19b). During the autopsy of Slab 4, pitting corrosion was observed in the top layer of reinforcement – in both the longitudinal bars and transverse wires – but was more pronounced in the transverse steel. In all cases, the corrosion was concentrated in the vicinity of the flexural cracks. The differences in the microstructure of the cold-worked wire and hot-rolled deformed reinforcement provide one explanation for the predominance of pitting corrosion in the transverse wires.

Connecting the steel sensing wire to the top layer of reinforcement was not successful in increasing the tributary area for the threshold sensors. However, the number of sensors that exceeded the corrosion threshold within the region of highest risk (Fig. 19a) did increase as the length of the exposure test increased. The frequency response of the passive sensors at the conclusion of the exposure tests is shown in Fig. 20 and 21 for Slabs 4 and 3, respectively.

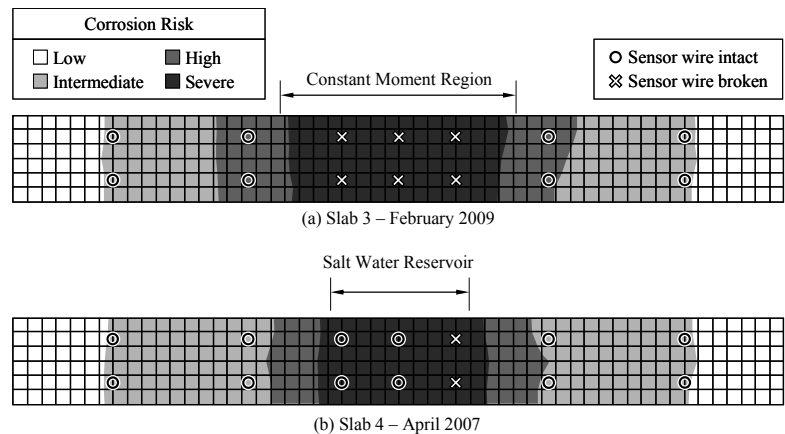
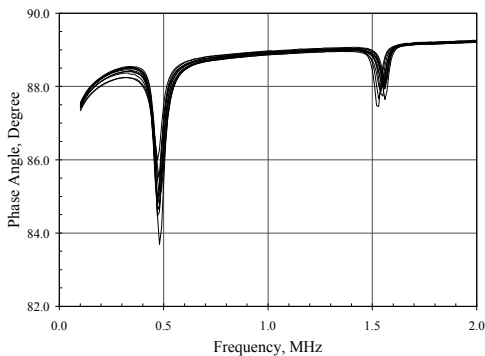
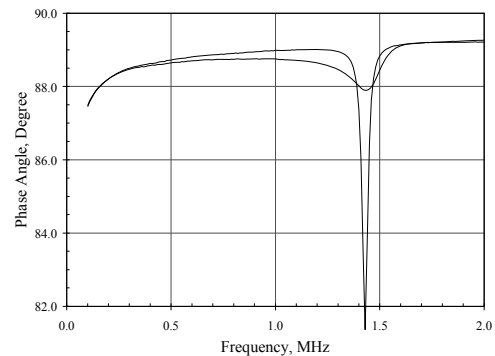


Figure 19: Contour plots of corrosion risk based on half-cell potentials and condition of sensors embedded in Slabs 3 and 4 at conclusion of long-term exposure test.

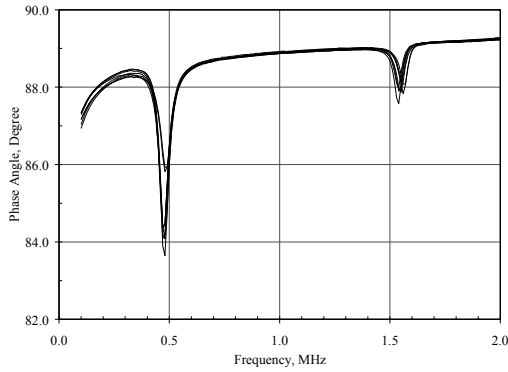


(a) Twelve sensors with intact sensing wires

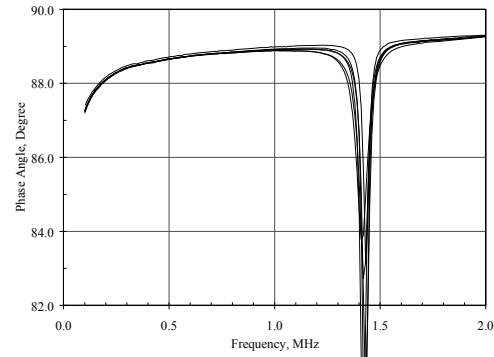


(b) Two sensors with corroded sensing wires

Figure 20: Response of sensors embedded in Slab 4 in April 2007.



(a) Eight sensors with intact sensing wires



(b) Six sensors with corroded sensing wires

Figure 21: Response of sensors embedded in Slab 3 in February 2009.

6. SUMMARY

The sensors discussed in this paper were designed to detect the onset of corrosion in reinforced concrete and prestressed concrete structures. The results from the exposure tests demonstrate that the passive, threshold sensors provide an economic, nondestructive means of evaluating the environmental conditions within a reinforced concrete structure. The condition of the external sensing wire is easily determined from the resonant frequencies of the wireless sensors. The presence of two dips in the phase response indicates that corrosion has not occurred at the location of the sensor, while a single dip indicates that a threshold amount of corrosion has occurred. Sensor output was not sensitive to environmental conditions, such as temperature, humidity, and the moisture content of the concrete. In addition, once corrosion was detected by a sensor, the readings did not reverse during a later interrogation. The only change in the sensor readings was caused by corrosion of the sensing wire.

The primary limitation of the wireless sensors is that the sensing area is quite small. Therefore, the threshold sensors must be considered to be point sensors, which only provide information about the conditions in the immediate vicinity of the sensor. Attempts to increase the tributary area of the sensors by providing an electrical connection between the reinforcement and the sensing wire were not successful. However, in all cases where the sensors indicated that a threshold amount of corrosion had occurred during the exposure test, the presence of corrosion was later confirmed during an autopsy. In addition, as the duration of the exposure test increased, variations in the readings of adjacent sensors that were subjected to the same environmental conditions decreased.

ACKNOWLEDGMENTS

The contributions of former graduate students Mathew M. Andringa, Nathan P. Dickerson, Kristi M. Grizzle, Lisa J. Novak, John M.H. Puryear, and Jarkko T. Simonen are gratefully acknowledged. Randall W. Poston, WDP and Associates, and Harovel G. Wheat, Department of Mechanical Engineering, University of Texas, also made significant contributions to the research. The research activities described in this paper were sponsored by the National Science Foundation through grant number CMS-0329808 to the University of Texas at Austin. The cognizant program officer was S.C. Liu. Early stages of the research were funded by the Texas Higher Education Coordinating Board through the Advanced Technology Program. The opinions expressed in this paper are those of the researchers and do not necessarily represent those of the sponsors.

REFERENCES

1. Ramsey, K.L. (2005). "Monitoring and Mitigation of Stay-Cable Vibrations on the Fred Hartman and Veterans Memorial Bridges, Texas," *Journal of the Transportation Research Board*, CD 11-S, Transportation Research Board, Washington, DC, pp. 547-555.
2. Çelebi, M. (2006). "Real-Time Seismic Monitoring of the New Cape Girardeau Bridge and Preliminary Analysis of Recorded Data: An Overview," *Earthquake Spectra*, Vol. 22, No. 3, pp. 609-630.
3. Simonen, J.T., Andringa, M.M., Grizzle, K.M., Wood, S.L., and Neikirk, D.P., "Wireless sensors for monitoring corrosion in reinforced concrete members," *Proceedings of SPIE*, Vol. 5391, 2004.
4. Dickerson, N.P., Simonen, J.T., Andringa, M.M., Wood, S.L., and Neikirk, D.P., "Wireless low-cost corrosion sensors for reinforced concrete structures," *Proceedings of SPIE*, Vol. 5765, 2005.
5. Dickerson, N.P., Andringa, M.M., J.M. Puryear, Wood, S.L., and Neikirk, D.P., "Wireless threshold sensors for detecting corrosion in reinforced concrete structures," *Proceedings of SPIE*, Vol. 6174, 2006.
6. Puryear, J.M.H., Andringa, M.M., Wood, S.L., and Neikirk, D.P., "Reliability of low-cost wireless sensors for civil infrastructure," *Proceedings of SPIE*, Vol. 6529, 2007.
7. ASTM G109, Standard Test Method for Determining the Effects of Chemical Admixtures on the Corrosion of Embedded Steel Reinforcement in Concrete Exposed to Chloride Environments, ASTM International, West Conshohocken, PA, 2005.
8. Dickerson, N.P., "Wireless corrosion sensors for reinforced concrete structures," *M.S. Thesis*, Department of Civil Engineering, University of Texas, August 2005. (available at <http://fsel.engr.utexas.edu/publications/>)
9. Puryear, J.M.H., "Passive, wireless corrosion sensors for reinforced concrete structures," *M.S. Thesis*, Department of Civil, Architectural, and Environmental Engineering, University of Texas, August 2007. (available at <http://fsel.engr.utexas.edu/publications/>)
10. Andringa, M.M., "Unpowered wireless sensors for structural health monitoring," *Ph.D. Dissertation*, Department of Electrical and Computer Engineering, University of Texas, December 2006.